https://doi.org/10.5194/egusphere-2025-6202
Preprint. Discussion started: 10 February 2026
© Author(s) 2026. CC BY 4.0 License.

Mantle Deformation Patterns Beneath the Central India Tectonic Zone: Evidence from SK(K)S Splitting Measurements in the Satpura Gondwana Basin and Adjacent Areas

Nitarani Bishoyi [1], Arun Kumar Dubey [1], and Ashwani Kant Tiwari [1]

[1]Department of Earth and Environmental Sciences, Indian Institute of Science Education and Research Bhopal - 462066, India

Correspondence: Ashwani Kant Tiwari (aktiwari@iiserb.ac.in)

Abstract. This study presents shear wave splitting (SWS) estimates for core-refracted SK(K)S phases utilizing data from nine seismic stations in the Central Indian Tectonic Zone (CITZ) that were temporarily operational between July 2023 and July 2025. The CITZ was formed during the Mesoproterozoic orogeny in central India, resulting from the collision of the northern Bundelkhand Craton with a jumble of South Indian cratons. We used rotation-correlation and transverse energy minimization methodologies to ascertain the SWS parameters, the fast polarization directions (FPDs) and splitting delay times (δt). A total of 129 high-quality SWS measurements were obtained from 87 earthquakes (M>5.5) at epicentral distances between 84°-145° for SKS phases and 84°-180° for SKKS phases. The mean δts at each seismic station ranges from 0.7 to 1.4 seconds, demonstrating the upper mantle heterogeneity in the study region. Most stations show NE-SW FPDs, aligning with the Absolute Plate Motion (APM) of the Indian plate. The difference between mean FPD and APM direction at some stations suggests the presence of fossilized anisotropic fabrics resulting from prior subduction events during the Mesoproterozoic Era. Seismic stations near the Deccan Volcanic Province and mantle dyke zones have lower δt (<1 second) values, indicating significant magmatism during the Cretaceous period. Our findings suggest that the mantle flow beneath the CITZ is affected by both the present APM direction of the Indian plate and lithospheric frozen anisotropy resulting from prior Mesoproterozoic orogeny and Cretaceous mantle plume activity.

1 Introduction

The Earth's mantle, a dynamic and heterogeneous layer, is critical to the geodynamic evolution of our planet. Understanding its deformation patterns is essential for unraveling the tectonic history and present-day geodynamics of any region. The tectonic history of the Indian landmass spans the formation of ancient cratons, incorporation into supercontinents such as Rodinia and Gondwana, and eventual collision with Eurasia (Rao and Reddy, 2002; Rogers and Santosh, 2003, 2009; Mandal et al., 2013), resulting in some of the most prominent geological features. Geochronological, geological, and paleomagnetic data suggests that multiple continental blocks came together during the Proterozoic era, leading to the formation of two major supercontinents (Zhao et al., 2004). The first, Columbia, formed around 1.8 billion years ago (Hou et al., 2008), while the second, Rodinia, emerged around 1.0 billion years ago (Li et al., 2008). One significant feature of these ancient tectonic events within the Indian shield is the presence of a Mesoproterozoic orogenic belt that runs in the ENE-WSW direction (Acharya, 1997;

https://doi.org/10.5194/egusphere-2025-6202
Preprint. Discussion started: 10 February 2026
© Author(s) 2026. CC BY 4.0 License.

Acharyya, 2003). This collisional zone, known as the Central Indian Tectonic Zone (CITZ) or Satpura Orogen, is an important suture zone where continental fragments collided and amalgamated during the Mesoproterozoic Era.

The CITZ is a suture zone that demarcates the boundary between the northern and southern Indian cratons (Figure 1). It originated during the Mesoproterozoic orogeny in central India, when the northern Bundelkhand Craton collided with a disordered group of South Indian cratons (Bastar, Dharwar, and Singhbhum cratons) (Radhakrishna and Ramakrishnan, 1988; Radhakrishna, 1989; Radhakrishna and Naqvi, 1986; Tewari, 2001). However, the accretion timing and subduction direction between the northern and southern Indian cratons are still debated Bhowmik et al. (2012); Roy and Prasad (2003); Bora and Kumar (2015). Some hypotheses propose that the southern Indian craton subducted northward beneath the northern Indian craton (Roy and Prasad, 2003; Mall et al., 2008; Mandal et al., 2013; Chattopadhyay et al., 2017), while others propose the opposite, with the northern Indian craton subducting southward beneath the southern Indian craton (Yedekar et al., 1990; Acharyya, 2003; Bora and Kumar, 2015). Furthermore, recent research has shown the likelihood of double-sided subduction in the central region (Naganjaneyulu and Santosh, 2010; Deshmukh and Prabhakar, 2020), which would involve processes such as slab breakoff and subduction polarity reversal. It has been a focal point of several tectonic activities, including continental collision, subduction, and mantle deformation.

The Central Indian Suture (CIS) and the Southeast Sakoli Shear (SES) form the southern limit of the CITZ, while the Son Narmada North Fault (SNNF) defines the northern boundary (Figure 1). The numerous main faults that exist within these borders are the Son Narmada South Fault (SNSF), Barwani Sukta Fault (BSF), Gavligarh Fault (GF), Tapti Fault (TF), and Tan Shear (TS) (Figure 1, Kaila and Krishna (1992); Narula et al. (2000); Bhandari et al. (2011)). These fault systems highlight the dynamic character of tectonic interactions and accompanying deformation within the CITZ, contributing to the evolving structural framework of this geologically active zone. Three prominent supracrustal belts - the Mahakoshal Supracrustal Belt, Betul Supracrustal Belt, and Sausar Supracrustal Belt - are exposed from north to south within these fault zones (Figure 2, Bhowmik (2019)). In addition to these supracrustal belts, the CITZ is home to a variety of lithological units, including intrusive granitoids from Dongargarh and Malanjkhand and rock formations from the Khairagarh, Nandgaon, and Chilpi Groups (Figure 2, Roy et al. (2002); Shukla et al. (2021)). This region features exposed Proterozoic basins, such as the Vindhyan basin, as well as rock sequences from the Gondwana Supergroup, Deccan Traps, and Quaternary alluvium (Figure 2).

Seismic anisotropy, caused by the directional dependence of seismic wave velocities, can be used to effectively define crustal and upper mantle deformation (Bowman and Ando, 1987; Vinnik et al., 1989; Silver and Chan, 1991; Savage, 1999). This anisotropy is typically linked to the deformation-induced alignment of anisotropic minerals such as olivine, orthopyroxene, and clinopyroxene in the upper mantle, which results from deformation processes such as lattice-preferred orientation (LPO) (Barruol and Mainprice, 1993) caused by mantle flow and tectonic stresses at plate boundaries. A shear wave splitting (SWS) analysis of SK(K)S core-refracted phases is used globally to quantify mantle anisotropy. The SWS occurs when a shear wave travels across an anisotropic medium, splitting into two orthogonal components. One component is aligned with the fast

https://doi.org/10.5194/egusphere-2025-6202
Preprint. Discussion started: 10 February 2026
© Author(s) 2026. CC BY 4.0 License.

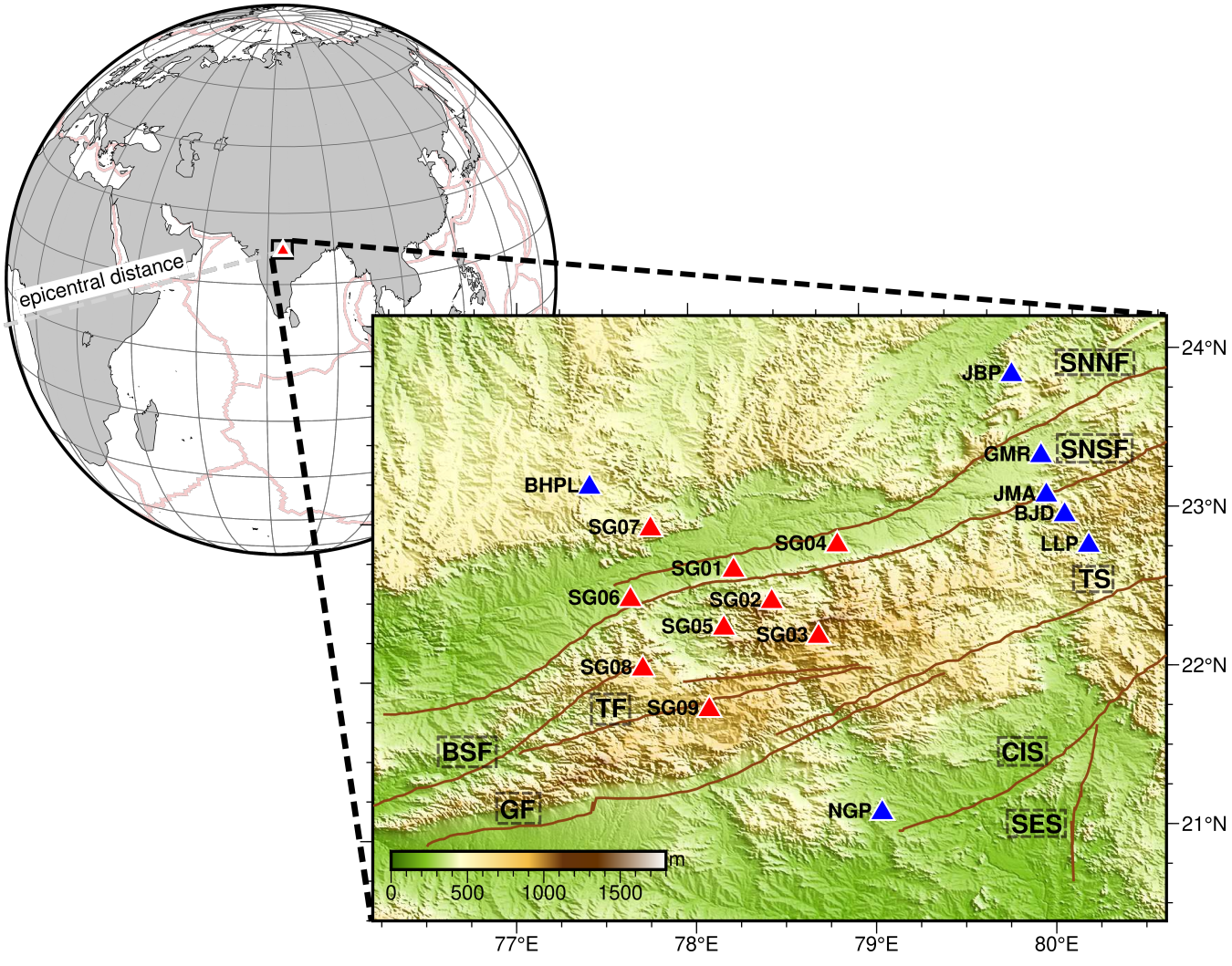


Figure 1. Tectonic and topographic map of the Central Indian Tectonic Zone across the Satpura Gondwana Basin. Red triangles denote the temporary seismic stations installed in and around the Satpura Gondwana Basin, whereas blue triangles show the permanent seismic stations in India controlled by the National Center for Seismology (NCS). BSF: Barwani Sukta Fault; CIS: Central Indian Suture; GF: Gavligarh Fault; SNNF: Son Narmada North Fault; SNSF: Son Narmada South Fault; TF: Tapti Fault; TS: Tan Shear; SES: Sakoli East Shear.

https://doi.org/10.5194/egusphere-2025-6202
Preprint. Discussion started: 10 February 2026
© Author(s) 2026. CC BY 4.0 License.

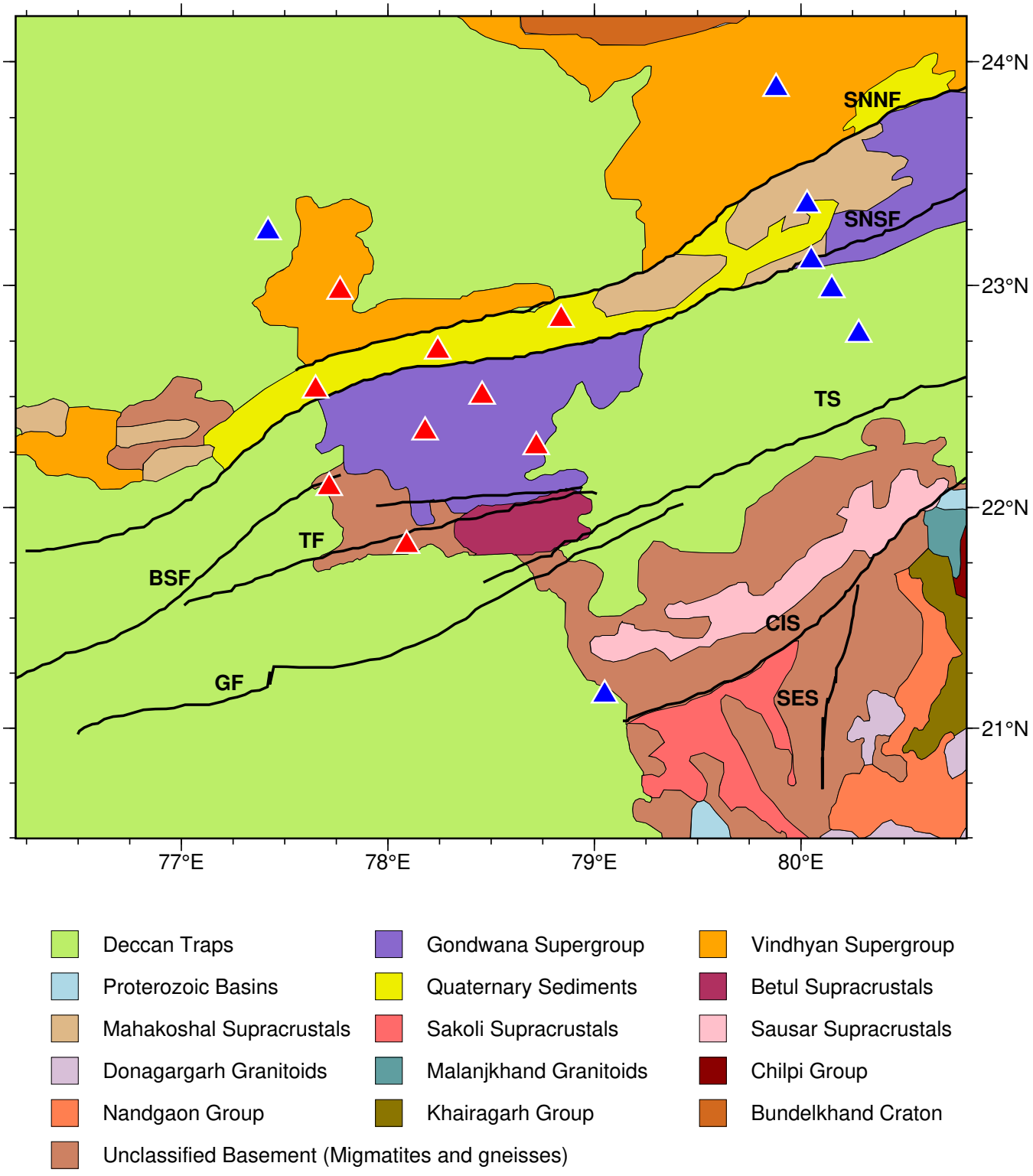


Figure 2. Geological map of the study region, with our seismic stations shown in red. The figure legend highlights various hues according to the names of geological provinces. This map is modified from Ramachandra and Roy (2001), Roy et al. (2002), and Shukla et al. (2021).

https://doi.org/10.5194/egusphere-2025-6202
Preprint. Discussion started: 10 February 2026
© Author(s) 2026. CC BY 4.0 License.

direction of the anisotropic structure and moves parallel to it, while the other component is perpendicular and moves in the slow direction. Seismic anisotropy analysis provides critical information regarding strain patterns, mantle flow, and the mechanical behavior of the lithosphere and sub-lithospheric system on the receiver side, allowing for inferences about mantle convection and past tectonic events.

A multitude of seismological investigations have been performed to elucidate the evolution and formation mechanisms of various regions in India by examining seismic anisotropy (Kumar and Singh, 2008; Paul et al., 2017; Biswal et al., 2020; Jana et al., 2021; Roy et al., 2021; Kanaujia and Surve, 2024; Roy et al., 2024) and its direct correlation to mantle deformation patterns, whether arising from present-day plate motion or the cumulative impact of prior and present-day orogenic events. Shear wave splitting has been extensively studied in the Himalayan region (northern India) to comprehend crustal and mantle deformation linked to the India-Eurasia collision (Paul et al., 2017; Kanaujia et al., 2019; Biswal et al., 2020). Similarly, numerous research studies on seismic anisotropy and its implications for lithospheric deformation have been performed in southern India (Roy et al., 2012; Kumar et al., 2015b; Sivaram et al., 2022) to better understand the evolution and formation mechanism of the southern Indian cratons. The SWS study has also highlighted the geological complexities of northeastern and eastern India (Bhukta et al., 2018; Singh et al., 2019). A recent study on seismic anisotropy across the whole Indian region (Roy et al., 2024) found that anisotropy in central India is caused by both frozen-in anisotropy and the shearing of the upper asthenosphere. Despite extensive research in these areas, the CITZ has received relatively less focus, despite its substantial importance. Due to a shortage of seismic stations, the region has minimal seismological data, and no extensive SWS study has been undertaken in this area (Figure 3). Figure 3 shows the previously conducted splitting measurements for all of India (represented by blue bars) alongside our study region (grey-shaded area), thereby addressing the data deficiency in central India. The CITZ region experienced subduction-accretion-collision tectonics during the Mesoproterozoic era and mantle plume activity during the Cretaceous period, resulting in the formation of Peninsular India (Mall et al., 2008; Mandal et al., 2013; Kumar et al., 2015a). Given its importance as a collisional zone, it is critical to investigate seismic anisotropy in this region to understand the deformation mechanisms.

This study examines teleseismic SK(K)S waveform data collected from nine temporarily deployed broadband seismic stations in the CITZ region to assess the seismic anisotropy of the upper mantle at each station. Two widely used splitting methods, rotation-correlation and transverse energy minimization, are employed to determine the SWS parameters, the fast polarization direction (ϕ or FPD) and delay time (δt). The resultant SWS parameters provide new insights into the deformational architecture of the crust and upper mantle in the study area. A comprehensive geodynamic model for the CITZ is presented to elucidate the observed SWS patterns, which reveal the tectonic context and mantle deformation mechanisms responsible for the anisotropy beneath the region.

https://doi.org/10.5194/egusphere-2025-6202
Preprint. Discussion started: 10 February 2026
© Author(s) 2026. CC BY 4.0 License.

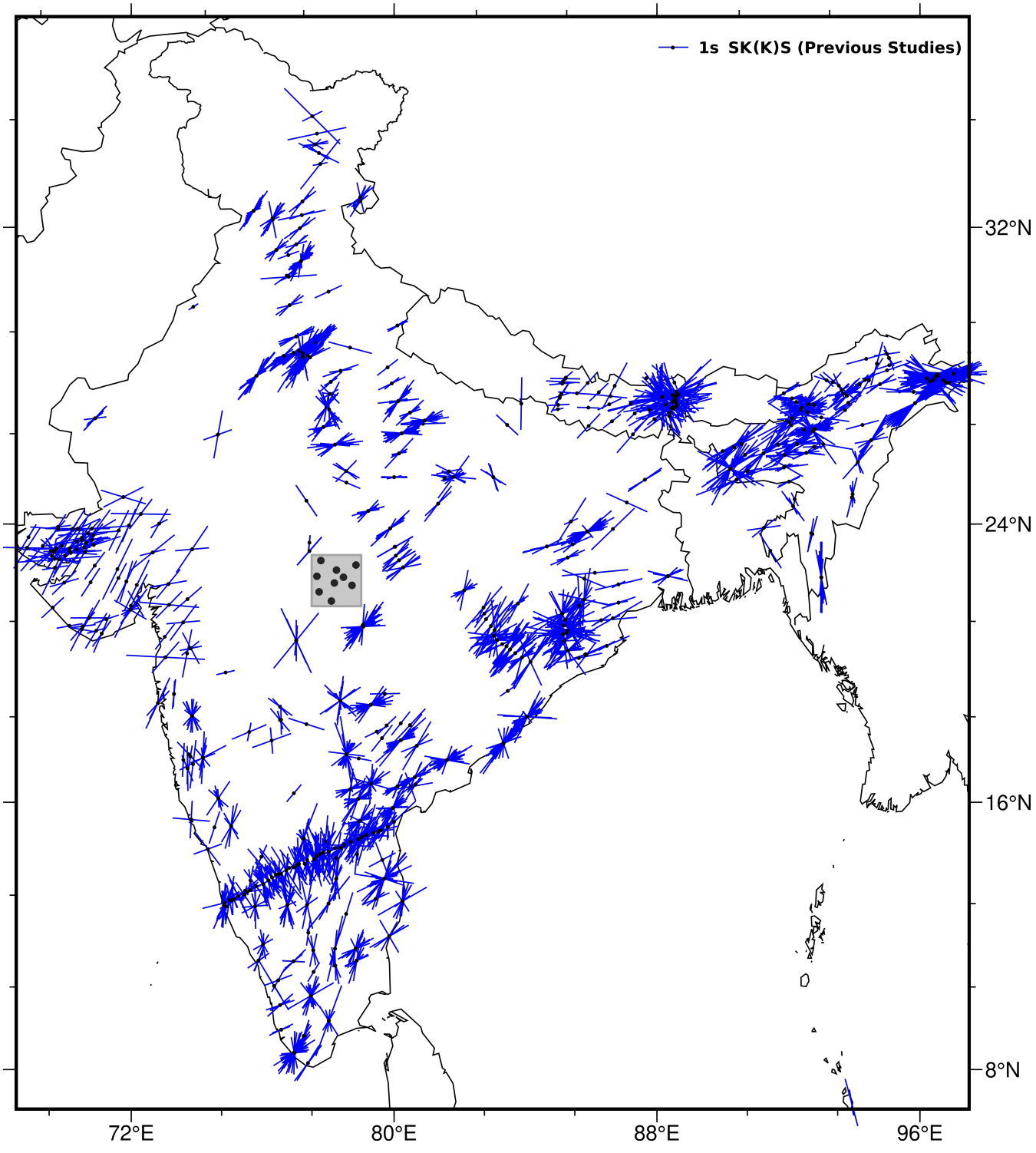


Figure 3. The figure illustrates the earlier SK(K)S-derived seismic anisotropy for the Indian region, depicted in blue (http://ds.iris.edu/spud/swsmeasurement), alongside our seismic stations, indicated in black circles. The bar length representing data at each seismic station corresponds to the δts , while their orientation indicates the FPDs.

https://doi.org/10.5194/egusphere-2025-6202
Preprint. Discussion started: 10 February 2026
© Author(s) 2026. CC BY 4.0 License.

2 Data and Methodology

We utilize broadband seismic data collected from nine portable seismic stations that were operational from July 2023 to July 2025 (Figure 1). The seismic stations, equipped with Trillium Compact broadband seismometers, were deployed in three phases, with three stations installed in each phase. The earthquakes, having magnitudes exceeding 5.5, have been chosen for the SKS phase occurring within the epicentral distance ranges of 84° - 145° and for the SKKS phase 84° - 180°, respectively (Figure 4). We have 424 teleseismic earthquakes based on magnitude and epicentral distance criteria, which were analyzed for SK(K)S-derived seismic anisotropy for all seismic stations. A band-pass filter having lower and higher cutoff frequencies of 0.05 Hz and 0.2 Hz, respectively, is subsequently employed to enhance the SK(K)S seismic phases.

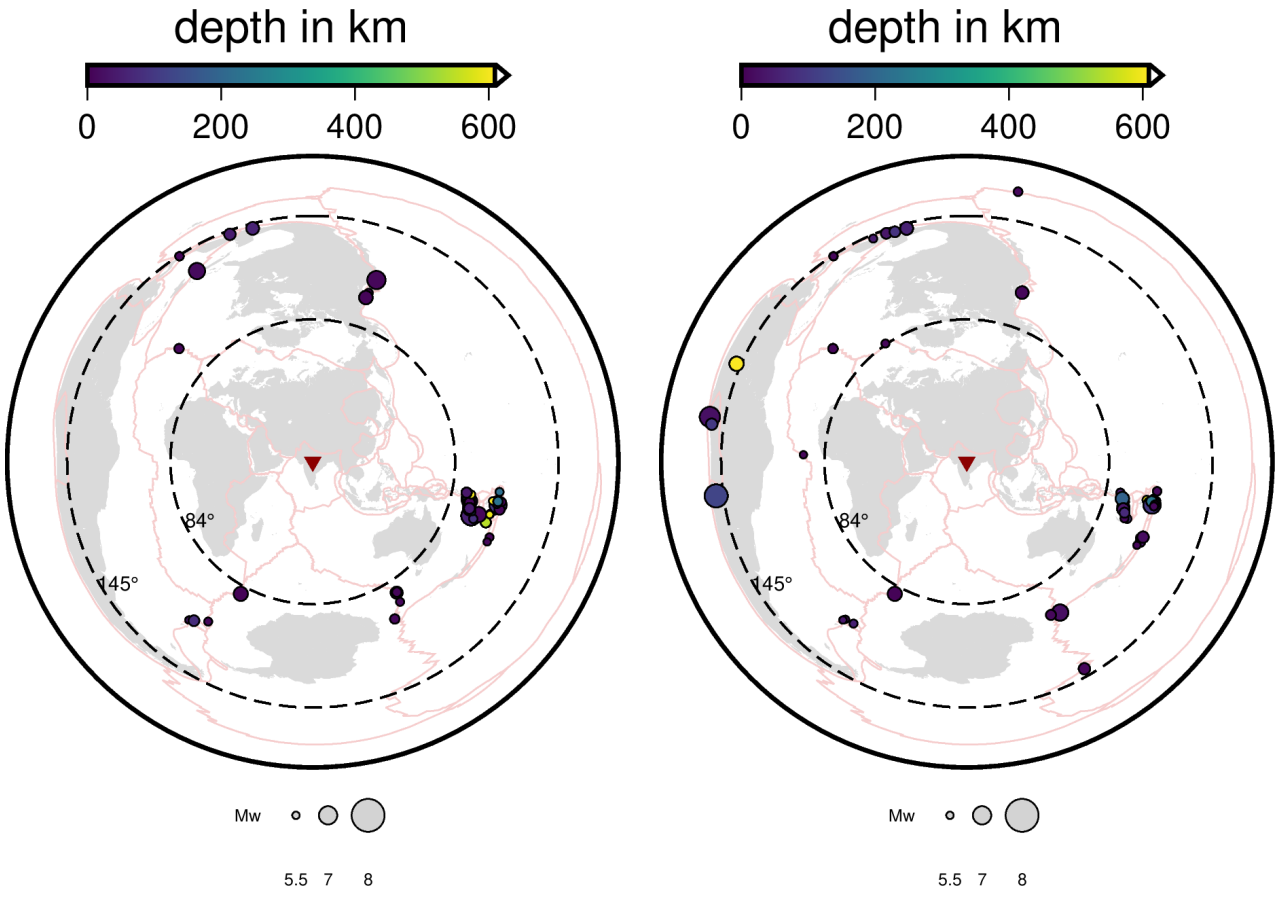


Figure 4. The epicentral distribution of earthquake events for (a) SKS (84° - 145°) and (b) SKKS (84° - 180°) seismic phases. The inverted dark red triangle represents the central location of seismic stations, while the circles denote earthquake events. The variation in circle colour indicates the depth of the earthquake events, while the size differences correspond to their magnitude.

https://doi.org/10.5194/egusphere-2025-6202
Preprint. Discussion started: 10 February 2026
© Author(s) 2026. CC BY 4.0 License.

The SWS measurements were performed using the SplitLab (Wüstefeld et al., 2008), a software package developed in MATLAB. SplitLab offers multiple splitting algorithms to determine the optimal SWS parameters, ϕ and δt. To ensure the reliability of SWS parameters, we employ two distinct and independent methodologies: rotation correlation and transverse energy minimization. The rotation correlation (RC) method (Bowman and Ando, 1987) determines the parameters ϕ and δt by finding the orientation that results in the highest correlation between the calculated fast and slow shear wave components. This method, however, may result in systematic inaccuracies, especially when the initial polarization aligns closely with the polarization of the fast or slow direction of the anisotropic media. Although predictable and well-documented, these errors can be accounted for to retrieve accurate splitting parameters.

The transverse energy minimization (TEM) technique (Silver and Chan, 1991) calculates ϕ and δt by minimizing the energy on the transverse component after applying the SWS correction. The TEM approach is generally considered more robust for SKS splitting measurements over a wide range of back azimuths. However, systematic errors, similar to those found in the RC approach, may have an impact, especially in circumstances with modest signal-to-noise ratios. This method assumes a single homogenous anisotropic layer and transverse isotropy with a horizontal symmetry axis. The TEM method follows a grid-search approach to ascertain the final optimal splitting parameters. It accounts for potential fluctuations, likely induced by data noise, by providing a confidence level for each splitting parameter. Consequently, the findings presented in this study are primarily based on the TEM method.

Figure 5 shows an example of the SKS-derived good splitting measurement recorded at station SG01. The high-quality split event demonstrates a corrected particle motion with a good overlap between the fast and slow components (Figure 5). Before correction, the particle motion exhibits an elliptical trajectory; however, after correction, it takes a linear path that corresponds to the back azimuth (Figure 5). The transverse energy nears zero in the adjusted transverse component plot, and the splitting parameters ϕ and δt are consistent, with ϕ agreeing within 10° across several methods and δt within 0.2 seconds (Figure 5). Figure 6 shows an example of the SKKS derived splitting measurements at stations SG01.

3 Results

After completing the splitting analysis, we have 129 reliable splitting measures, including 82 SKS splitting measurements and 47 SKKS splitting measurements. The majority of the analysed earthquakes are located in the back-azimuth range of 90° to 120°, as demonstrated by the back-azimuthal rose diagram of the final good quality splitting measures (Figure 7). Figure 7 shows a histogram of individual splitting parameters, demonstrating a predominant concentration of FPDs at 40° and δt around 0.85 - 1.1 seconds. The rose diagram for each split measurement (Figure 8) illustrates the variance and predominant orientation of FPDs at each seismic station.

https://doi.org/10.5194/egusphere-2025-6202
Preprint. Discussion started: 10 February 2026
© Author(s) 2026. CC BY 4.0 License.

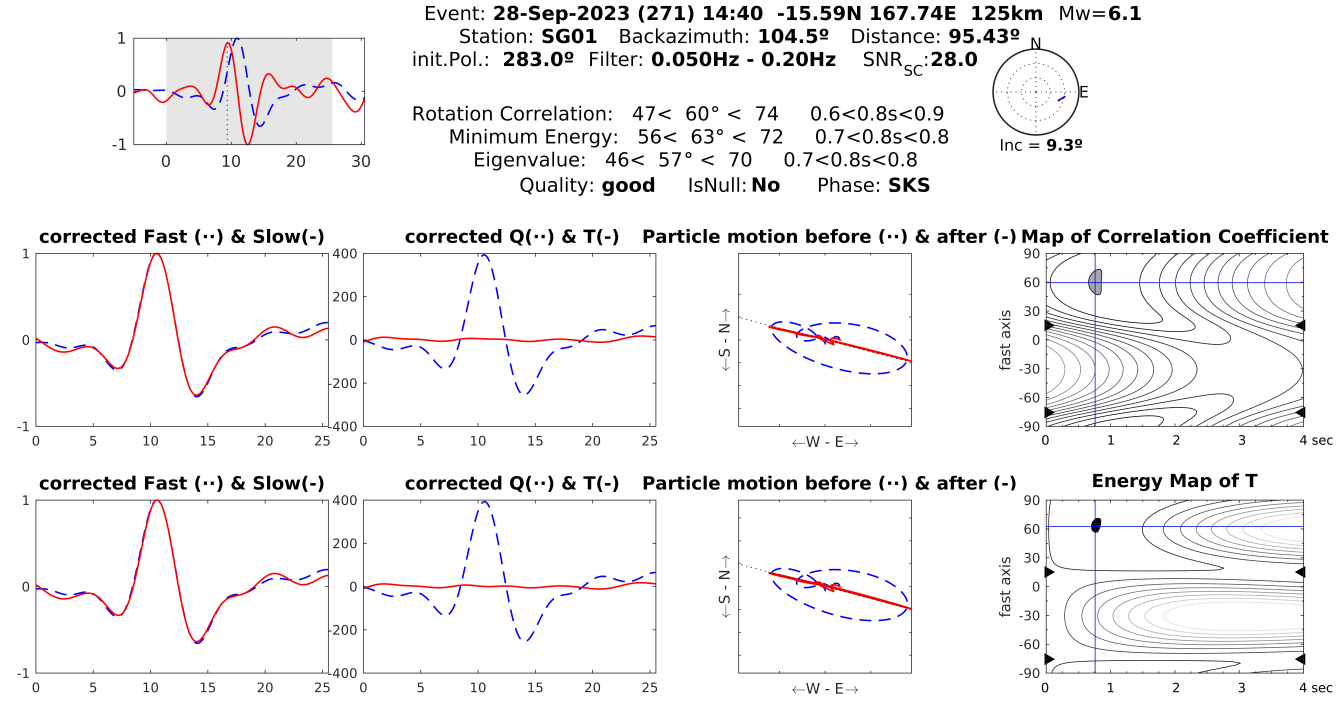


Figure 5. An example of a good SKS splitting phase for an earthquake recorded by the SG01 seismic station. The upper left graphic displays the radial component (blue dotted) and transverse (red solid) component, with the chosen time frame highlighted in gray. The top bar displays the event, station, and computed result information simultaneously. The stereoplot is shown in the top right corner. The second row presents the outcomes of the rotation-correlation (RC) method, including SKS fast directions (blue dashed) and slow ones (red solid) after RC delay correction; radial (blue dashed, Q) and transverse (red solid, T) components after RC delay correction; particle motion before (blue dashed) and after (red solid) RC delay correction; and a map of correlation coefficients. The third row displays the results of the transverse energy minimization technique. The descriptions are similar to the RC plots.

After calculating individual SK(K)S splitting measurements, the station-averaged splitting parameter for each station is calculated by averaging all splitting parameters derived from numerous events. The von Mises approach (Cochran et al., 2003) was used to calculate the circular mean of ϕ, whereas station-averaged δt was calculated using the arithmetic mean. The station-averaged SK(K)S splitting parameter for each seismic station is shown in Table 1. The average splitting δt at each station vary from 0.74 to 1.4 seconds (Figure 9). We have the lowest value of δt at the SG02 seismic station. Stations SG01, SG03, SG04, SG05, and SG08 show high anisotropy ($>$ 1 s), while stations SG02, SG06, SG07, and SG09 have low δt ($<$ 1 s). The FPD values across all stations range from 24.84° (SG06 seismic station) to 70.88° (SG03 seismic station). Most seismic stations have a predominant NE-SW alignment of FPDs, which correlates closely to the Absolute Plate Motion (APM) direction of the Indian Plate (Figure 10).

https://doi.org/10.5194/egusphere-2025-6202
Preprint. Discussion started: 10 February 2026
© Author(s) 2026. CC BY 4.0 License.

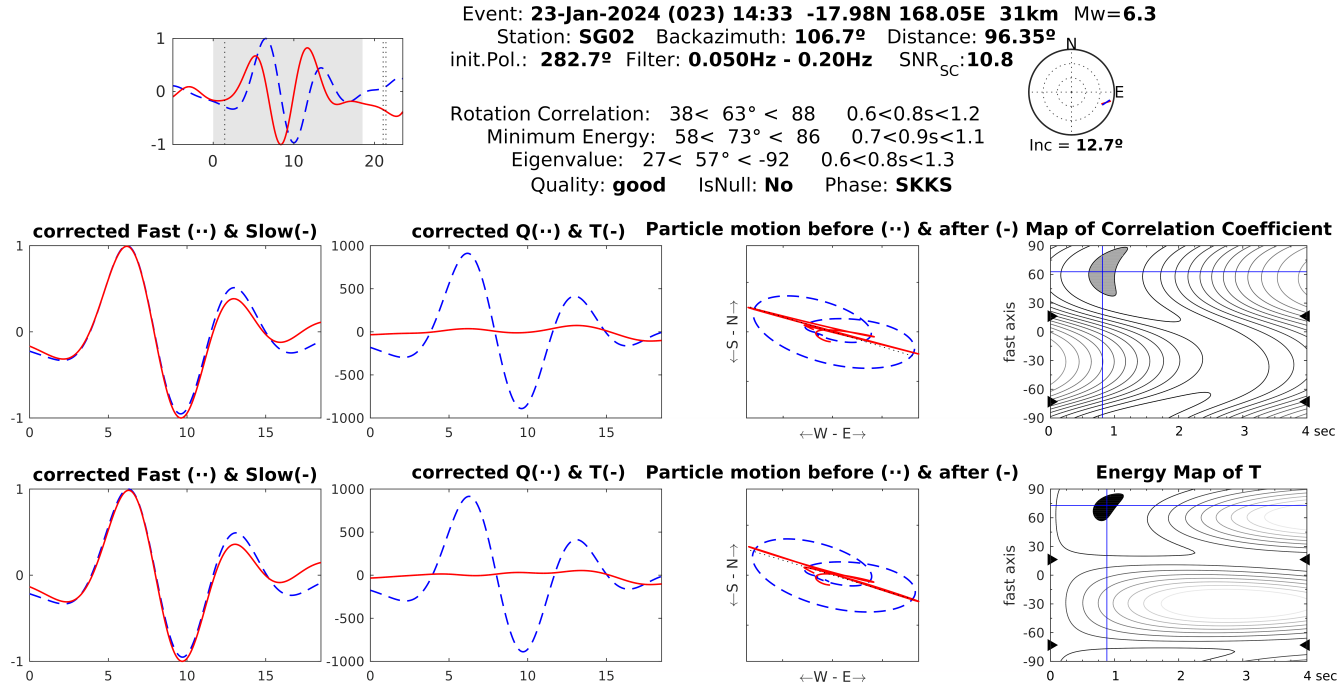


Figure 6. An instance of good SKKS splitting measurement for an event recorded by the SG02 seismic station. The description corresponds identically to Figure 5.

Table 1. Details of seismic stations, with averaged splitting parameters (FPD and δt)

Station	Lat (°)	Long (°)	Operation time		Station-averaged splitting parameters		No. of SK(K)S measurements
			Start date	End date	ϕ (°)	δt (s)	
SG01	22.70448	78.24171	16-07-2023	29-02-2024	43.90	1.08	13
SG02	22.50137	78.45606	17-07-2023	02-03-2024	56.49	0.74	19
SG03	22.27442	78.71826	18-07-2023	02-03-2024	70.88	1.04	13
SG04	22.84751	78.83887	02-03-2024	05-10-2024	34.61	1.42	16
SG05	22.34044	78.18029	03-03-2024	05-10-2024	47.70	1.29	19
SG06	22.52954	77.64957	03-03-2024	05-10-2024	24.84	0.90	15
SG07	22.97337	77.76826	06-10-2024	24-07-2025	59.66	0.88	10
SG08	22.08976	77.71605	05-10-2024	24-07-2025	64.22	1.03	12
SG09	21.82800	78.09055	05-10-2024	24-07-2025	51.64	0.95	12

https://doi.org/10.5194/egusphere-2025-6202
Preprint. Discussion started: 10 February 2026
© Author(s) 2026. CC BY 4.0 License.

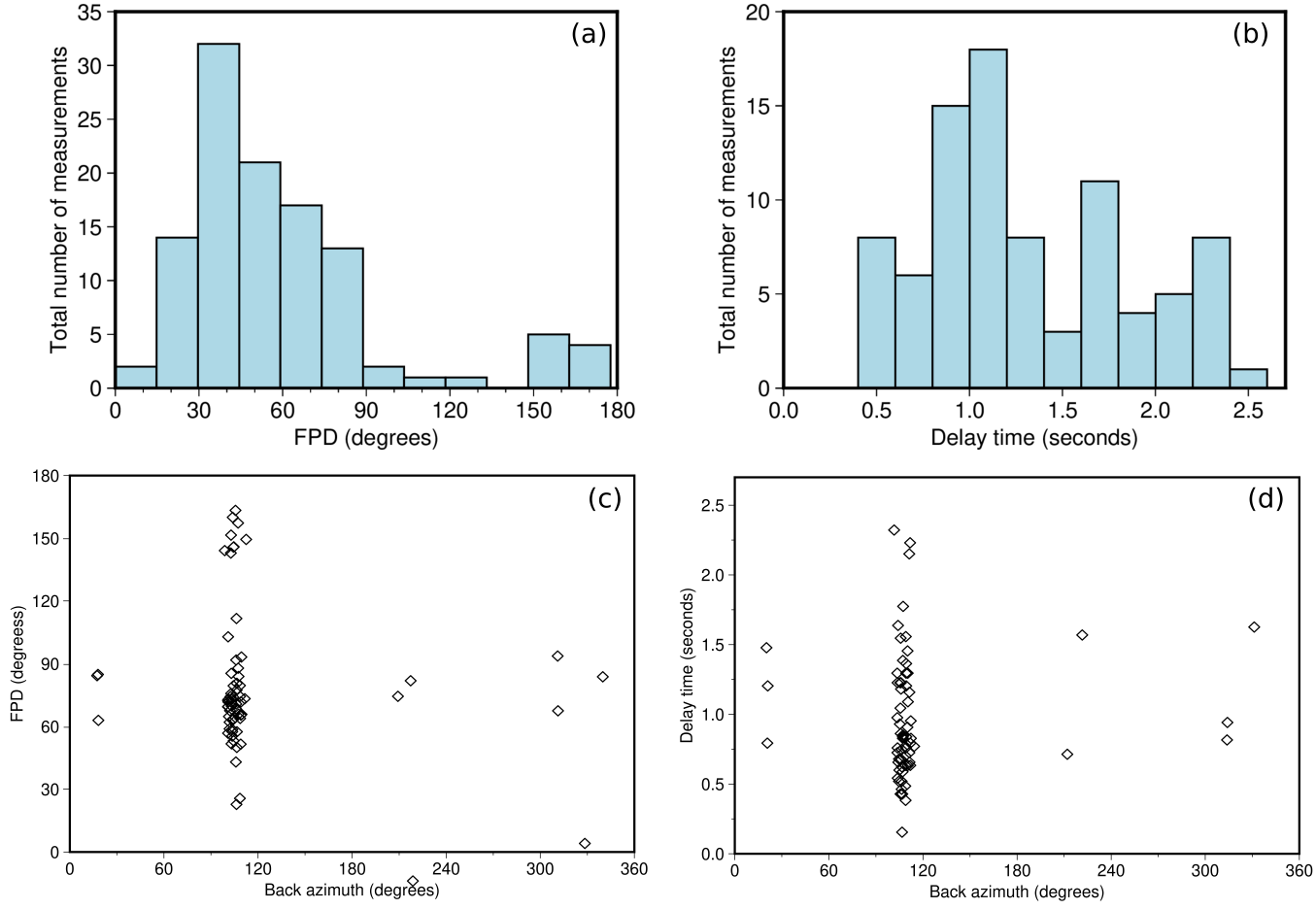


Figure 7. Histograms illustrating individual splitting parameters: (a) fast polarization directions (FPDs) and (b) delay times (δt). (c) and (d) illustrate the back azimuthal variation of individual FPDs and δts across all seismic stations, respectively. The majority of splitting measurements are concentrated within the backazimuthal range of 90° to 120°.

4 Discussion

4.1 Comparative Analysis of APM and Splitting Measurements

Understanding the deformation pattern is critical for studying the formation mechanisms and growth history of the CITZ region. The correlation between seismic anisotropy and geodetic measurements (APM and GPS velocity vectors) is critical for understanding deformation mechanisms in the crust and upper mantle. The GPS measurements pertain to deformation in the upper crust (Chen et al., 2013), whereas the APM is mostly about the upper mantle (Kreemer, 2009). The discrepancies between SK(K)S-derived FPDs and GPS data reveal differences in deformation patterns throughout the crust and upper mantle, while the absolute difference between FPDs and APM direction explains frozen-in anisotropy and mantle flow associated with the Indian plate. We combine our SK(K)S wave splitting measurements with prior GPS velocity vectors (Jade et al., 2017),

https://doi.org/10.5194/egusphere-2025-6202
Preprint. Discussion started: 10 February 2026
© Author(s) 2026. CC BY 4.0 License.

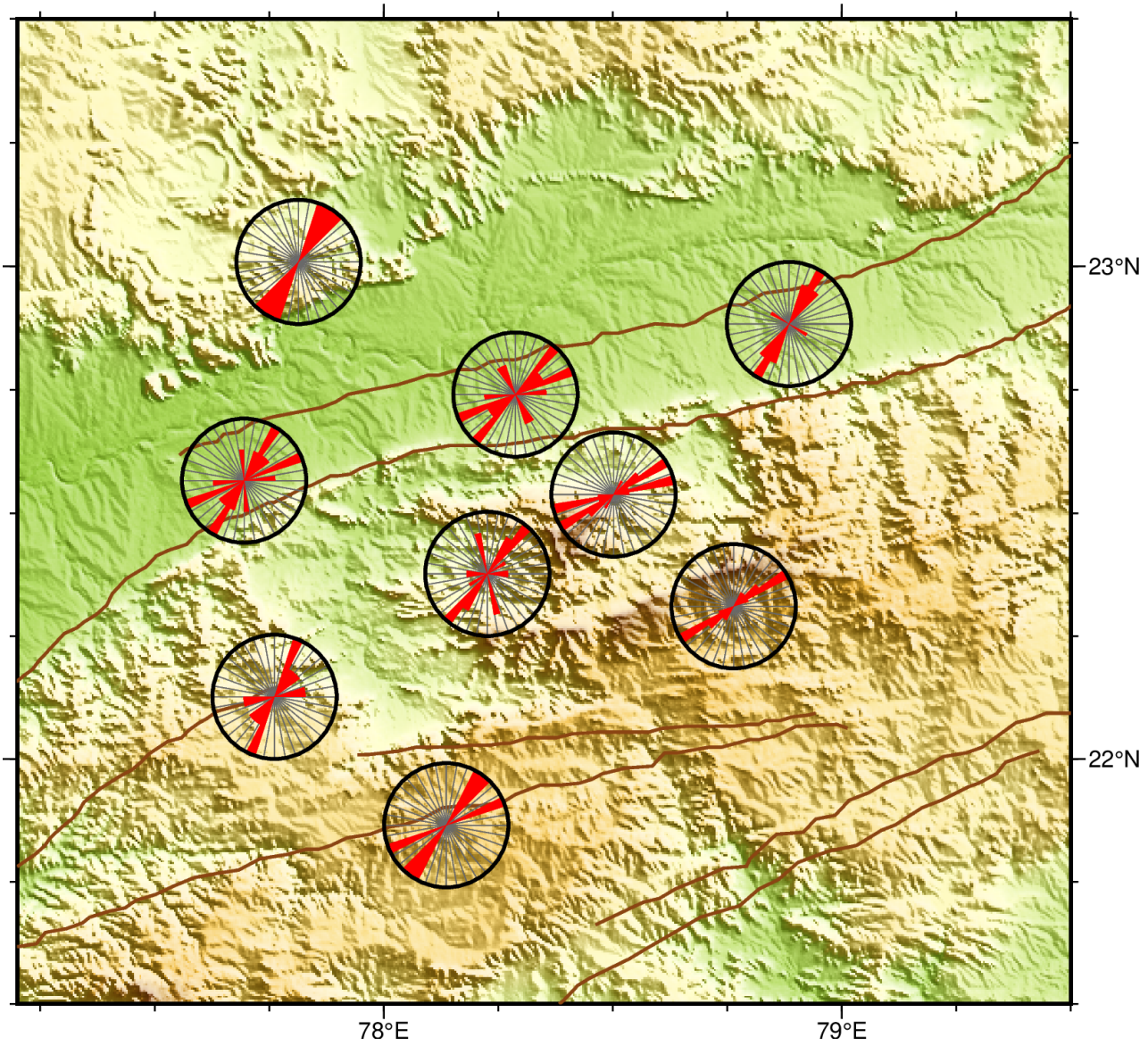


Figure 8. Rose diagrams depicting the distribution of individiual SK(K)S splitting outcomes at each station throughout the region.

https://doi.org/10.5194/egusphere-2025-6202
Preprint. Discussion started: 10 February 2026
© Author(s) 2026. CC BY 4.0 License.

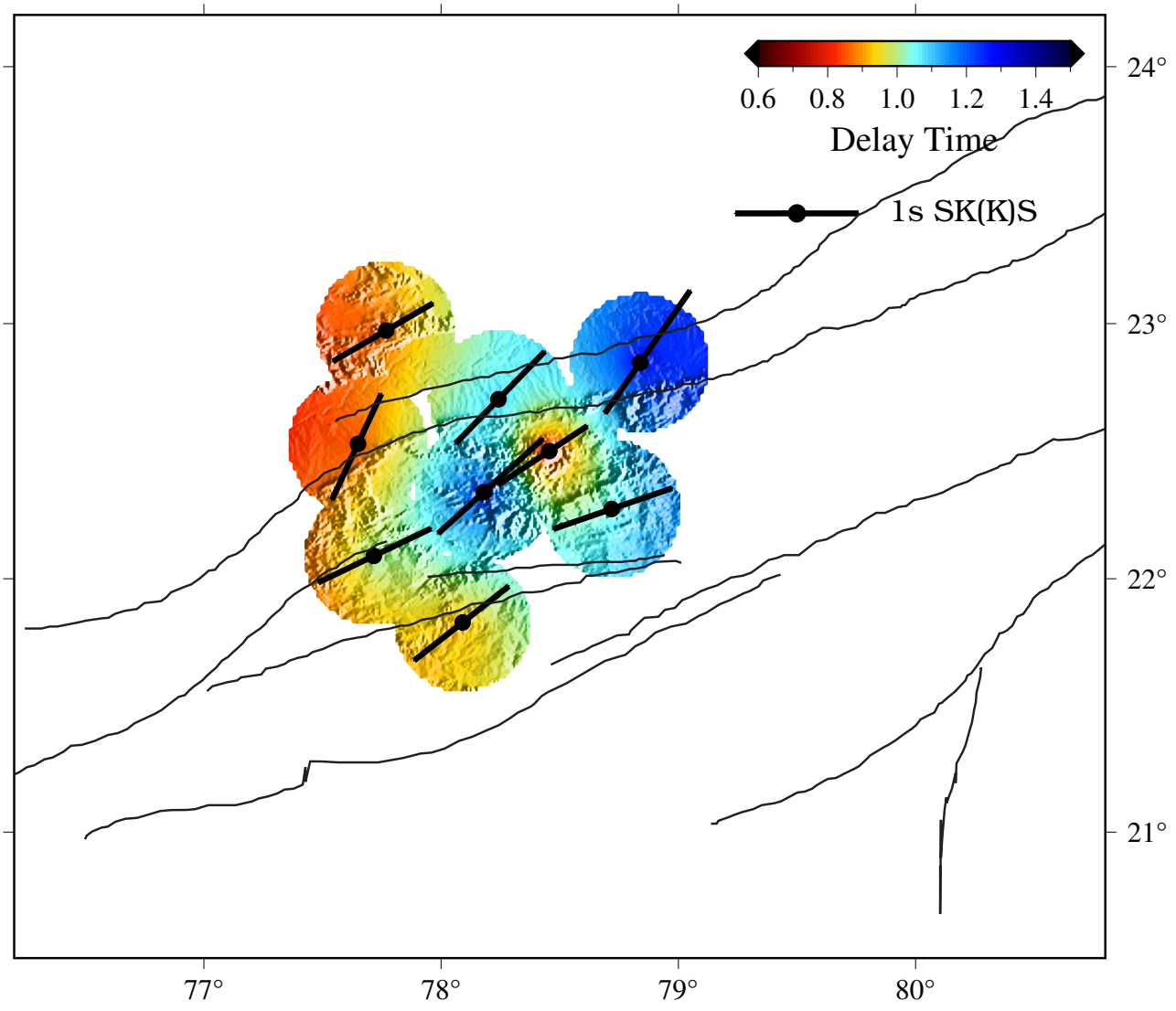


Figure 9. The tectonic map of the study area, which depicts the station-averaged SK(K)S wave splitting measurements. The azimuth of the solid black bars denotes the FPDs of the obtained splitting parameter. The interpolated split delay time at each station is presented in a color-coded format to illustrate lateral variations in delay times. The black circles indicate the seismic stations used in this study.

https://doi.org/10.5194/egusphere-2025-6202
Preprint. Discussion started: 10 February 2026
© Author(s) 2026. CC BY 4.0 License.

and APM velocity vectors obtained from UNAVCO's online platform (https://www.unavco.org/software/geodetic-utilities/plate-motion-calculator/plate-motion-calculator.html), which utilizes the ITRF2020 model (Altamimi et al., 2023). Figure 10 shows the station-averaged splitting parameters together with APM and GPS velocities throughout the study area, highlighting notable similarities and differences across GPS, APM velocities, and SK(K)S splitting data. GPS velocities align in a NE-SW direction, indicating that the northward movement of the Indian plate primarily affects crust motion in the study area (Figure 10). The GPS measurements and their comparison with the APM (Mahesh et al., 2012; Jade et al., 2017), show that the interior of the Indian plate, including areas influenced by the Narmada-Son lineament or other faults, exhibits no significant current deformation, and the lithosphere behaves as a rigid block. SK(K)S-wave splitting patterns indicate that complex mantle deformation beneath the CITZ, results from the interaction of lithospheric strain and mantle flow. A minor variance in FPD and APM (up to 10°) is noted at seismic sites SG01, SG02, SG05, SG07, and SG09 (Figure 11), indicating the predominance of asthenospheric flow. The significant absolute differences between station-averaged FPD and APM direction in the western region (26° at SG06 and 12° at SG08) and in the eastern region (16° at SG04 and 19° at SG03) indicate the influence of ancient orogenic events from the Mesoproterozoic era (Deshmukh and Prabhakar, 2020). The CITZ may act as a channel for lateral flow within the asthenosphere. This flow could have contributed to anisotropy signatures that left significant imprints in the lithosphere, revealing varying patterns of crustal and upper mantle deformation. The variations in FPDs across different stations imply varied orientations of stress and strain within the region, highlighting the historical shifts in tectonic stress fields.

4.2 Anisotropic Sources and Geodynamic Implications

The measurements of core-refracted SK(K)S phase splitting provide integrated anisotropy information from the mantle to the surface, impacted by both crustal and mantle anisotropy. Crustal anisotropy typically ranges between 0.1 and 0.3 seconds (Silver and Chan, 1991); however, the measured δts varies from 0.74 seconds at station SG02 to 1.4 seconds at station SG04, indicating that the primary source of seismic anisotropy lies inside the upper mantle. The considerable variation in FPD values, ranging from 24.84° at station SG06 to 70.88° at station SG03, suggests heterogeneous anisotropic structures in the mantle under the CITZ, which is caused by the combined influence of frozen-in anisotropy within the lithospheric mantle and the present plate motion of India. Along with the current research splitting measurements, Figure 10 displays prior measurements by Roy et al. (2021) and Roy et al. (2024) throughout the Indian shield, including stations BHPL, NGP, JEP, GMR, JMA, BJD, and LLP, which are shown in blue. Both fossilized anisotropy and asthenospheric flow have an impact on upper mantle anisotropy of the central Indian region Roy et al. (2024). Our findings for the majority of seismic stations are consistent with earlier studies, reaffirming the NE-SW anisotropy orientation. The observed lateral variations in anisotropic results indicate the presence of multiple sources of anisotropy within the region, which could be attributed to a dynamic interplay between lithospheric deformation and asthenospheric flow induced by regional plate motion. The frozen lithospheric deformation is associated with historical convergence and collisional orogeny during the Mesoproterozoic era, as well as mantle plume activity during the Cretaceous period which manifests on the surface as the Deccan Volcanic Province (DVP) and dykes (Deshmukh and Prabhakar, 2020). The splitting data may indicate a multilayered anisotropic structure; however, the limited depth resolution of the used methodologies, the short duration of seismic data, and the confined back-azimuthal range of earthquakes,

https://doi.org/10.5194/egusphere-2025-6202
Preprint. Discussion started: 10 February 2026
© Author(s) 2026. CC BY 4.0 License.

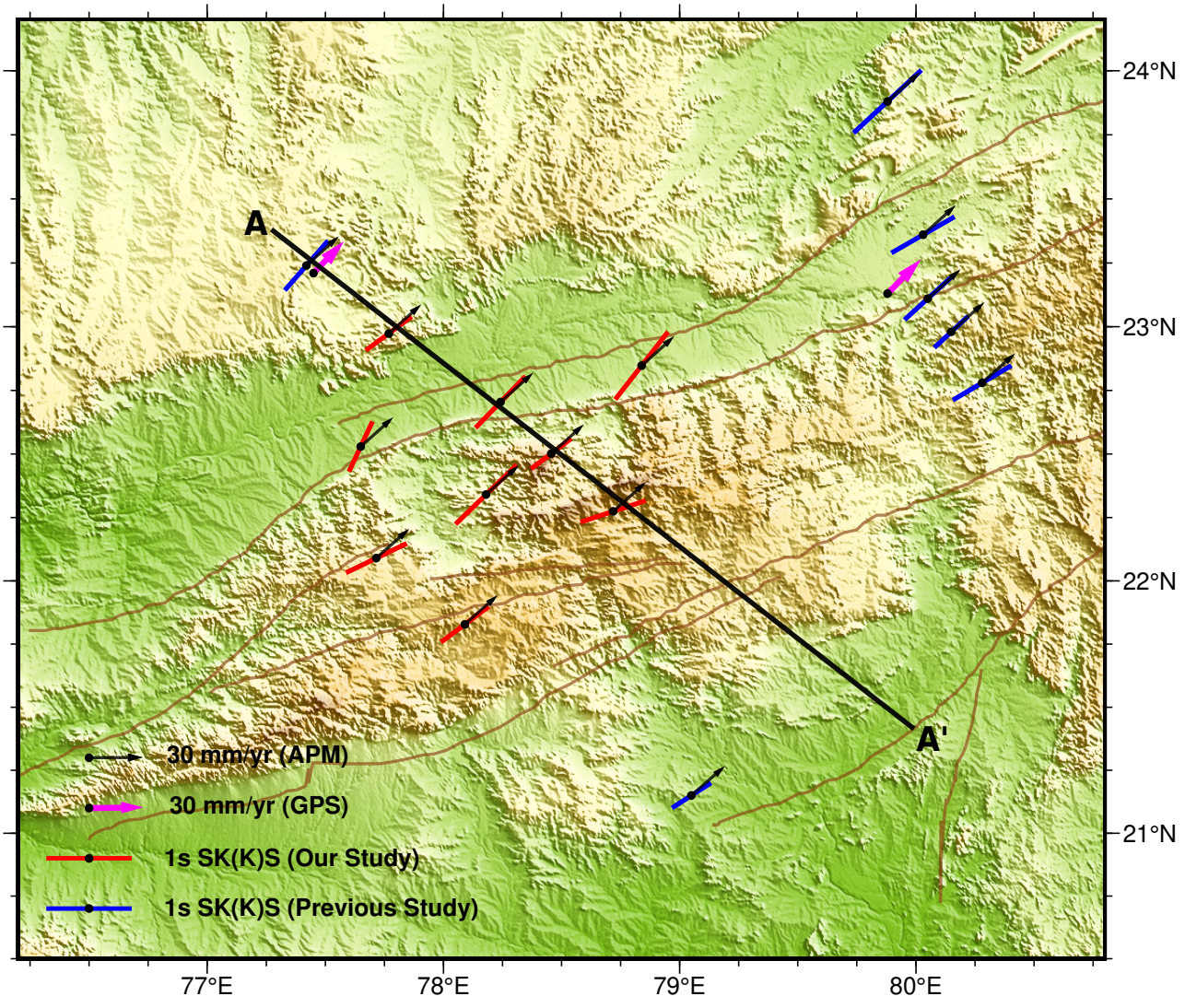


Figure 10. Lateral variation of the anisotropic and geodetic data illustrated on the tectonic and topographic map of the study region. The station-averaged splitting measurements for this study are depicted in red, whereas previous splitting measurements in adjacent regions are represented in blue. The black dots signify the location of the stations. The inclination of each bar represents the FPD, while the length denotes the δt. The GPS velocity vectors are depicted in magenta, whereas the APM direction of the Indian plate at each seismic station is represented in black.

https://doi.org/10.5194/egusphere-2025-6202
Preprint. Discussion started: 10 February 2026
© Author(s) 2026. CC BY 4.0 License.

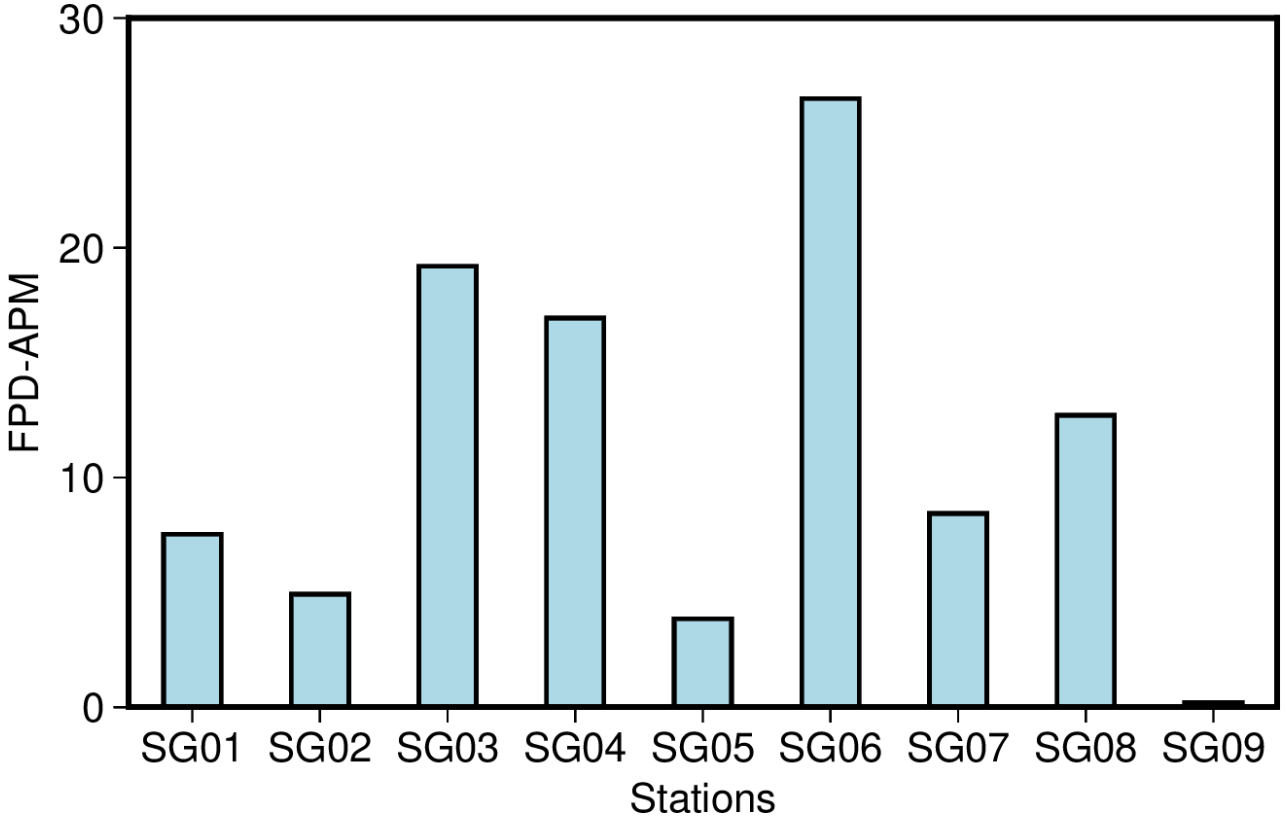


Figure 11. The bar diagram depicts the absolute difference between the station-averaged FPD for each station and the APM direction of the Indian plate, signifying the deviation of FPDs from the APM direction.

which are primarily concentrated in the southeast, make establishing a multilayered anisotropic model challenging.

The lithosphere-asthenosphere boundary (LAB) beneath central India has a non-uniform depth profile (Kumar et al., 2013), characterized by undulations that could indicate tectonic and compositional variations across the region. The undulating LAB may influence seismic wave propagation, resulting in diverse anisotropic signatures that depend on the boundary's depth and shape. In shallower LAB zones, mantle flow may have a greater direct influence on the anisotropic fabric, contributing to SWS with FPDs aligned with recent tectonic stress directions or mantle convection patterns (Bormann et al., 1996). The SG03 and SG06 seismic stations may be located in locations with thicker lithosphere, where fossilized fabric from past tectonic events could influence anisotropy (Melo et al., 2018; Yang et al., 2017). In the northeast of the study region, the stations JBP to LLP also exhibit a distinct splitting trend, demonstrating that lithospheric thickness is almost proportionate to δt (Roy et al., 2024). This trend is corroborated by Moho depth estimates from the passive seismological study of the Narmada Paleo rift (Kumar et al., 2015a), which show a duplex structure of the Moho discontinuity, characterized by a thicker crust (surpassing 52 km) within the rift zone than in surrounding regions. Regions with higher lithospheric thickness may have seen more intense defor-

https://doi.org/10.5194/egusphere-2025-6202
Preprint. Discussion started: 10 February 2026
© Author(s) 2026. CC BY 4.0 License.

mation, especially in active subduction and collision zones. Figure 12 shows that the central region of the study area has seen many stages of deformation resulting in higher δts. Stations SG07, SG06, and SG09, located within or near DVP, have lower δt values. Lower δt at these stations could be due to mantle plume upwelling in the upper Cretaceous to early Paleocene (Krishnamurthy, 2020). The lower δt (0.74 sec) at the Pachmarhi region (SG02 seismic station) is due to significant magmatism during the Cretaceous period in the Narmada and Tapti graben areas, as evidenced by the presence of dykes (Shukla et al., 2022). The 2D gravity modeling of the Satpura Gondwana basin (Singh et al., 2015) additionally demonstrated that the basin functioned as a drop-down basin before being uplifted to its current elevation by late Cretaceous Deccan volcanism. Anisotropic fabrics beneath SG04 and SG05 seismic stations show preserved mantle deformation from ancient subduction zones, as shown by elevated δt values.

The SG08 seismic station (SG08), located near the Tapti Fault, exhibits a fault-parallel FPD, suggesting uniaxial compression and a fault that may extend to greater depths (Savage, 1999), possibly reaching the lithospheric mantle. The Tapti fault is a major east-west trending structure located in central India (Chakraborty and Ghosh, 2005). The fault-parallel alignment of FPD suggests that seismic anisotropy in this area is structurally controlled by the fault, implying that it serves as a weak lithospheric zone influencing upper mantle deformation (Kumar et al., 2007). Fault-parallel FPD alignment suggests that the Tapti fault, which has undergone several reactivation stages in conjunction with present-day stress fields, has pre-existing weaknesses in the crust and mantle (Copley et al., 2014), and that the fault may be a deep-seated lithospheric-scale fault.

We created a conceptual tectonic model (Figure 12) to understand how CITZ formation over time affects deformation and impacted the FPD orientation and δts values. The model is made along AA', which stretches from a region of low deformation in the northwest to an active subduction zone in the southeast. This is corroborated by variations in SK(K)S-derived FPDs and δts. Stations SG01 and SG03 have higher δts compared to BHPL and SG07, indicating a greater impact from subduction-related deformation (Deshmukh and Prabhakar, 2020). The lower δt at station SG02 is attributed to significant magmatism during the Cretaceous period mantle plume activity, as shown by the existence of dykes in the Pachmarhi region. The mantle plume is inducing localized alterations in lithospheric structure and seismic anisotropy. The low δt at NGP is likely due to its considerable distance from the active subduction zone. Station SG03 exhibits significant variability in FPD and APM, reflecting a tectonically complex mantle deformation zone linked to the inherited frozen lithospheric anisotropy resulting from previous convergence and collisional orogeny beneath the CITZ region, in addition to the current APM direction of the Indian plate. The recent tectonic evolution model of the CITZ (Deshmukh and Prabhakar, 2020, and references therein) proposes the likelihood of double-sided subduction, which accounts for the present-day tectonic framework of the CITZ region. This involves the processes of slab roll-off and subduction polarity reversal between the northern and southern Indian cratons, characterized by an initial southward subduction of the northern Indian craton, followed by a reversal of the subduction polarity. However, the current investigation of seismic anisotropy does not provide confirmation of the slab break-off hypothesis. To obtain comprehensive information regarding the detached remnants slab, slab break-off, and polarity reversal, additional seismological investigations (such as seismic tomography, splitting intensity tomography, receiver function analysis, etc.) are required to

https://doi.org/10.5194/egusphere-2025-6202
Preprint. Discussion started: 10 February 2026
© Author(s) 2026. CC BY 4.0 License.

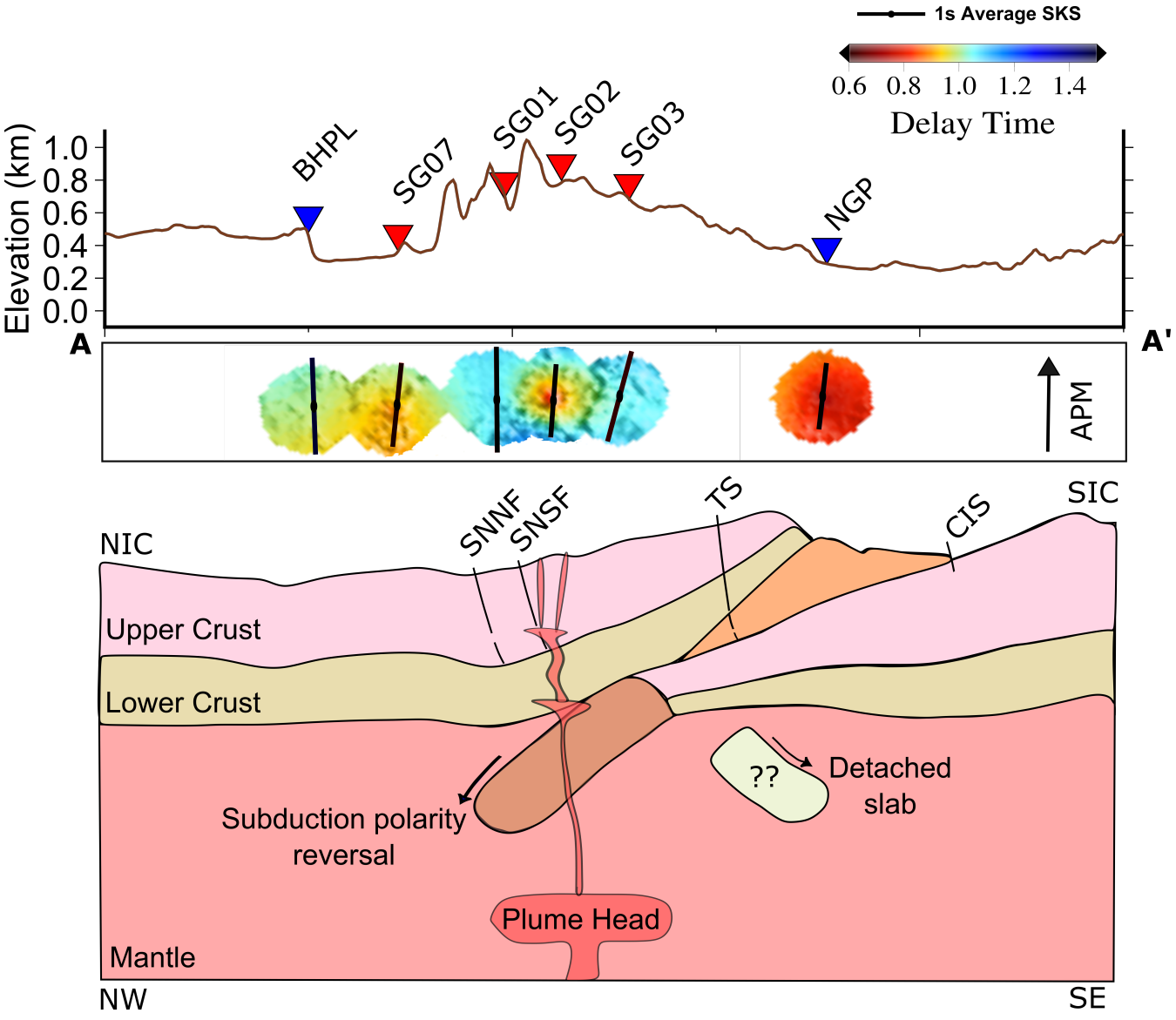


Figure 12. A hypothetical model (not to scale) depicting all tectonic events that have influenced the formation of CITZ over time and affected the FPD alignment and δts. The model is built along AA' profile, extending from a low deformation area in the northwest to an active subduction zone in the southeast, as illustrated in Figure 10. The subduction model is modified from Deshmukh and Prabhakar (2020) and Mall et al. (2008), while the plume upwelling is additionally demonstrated by Shukla et al. (2022). The black bars represent the station-averaged FPD, with the length indicating the δt of our findings and prior research. The interpolated split delay time at each station is displayed in a color-coded style to distinctly illustrate lateral variations in split delay times. APM: Absolute Plate Motion, NIC: North Indian Craton, SIC: South Indian Craton.

https://doi.org/10.5194/egusphere-2025-6202
Preprint. Discussion started: 10 February 2026
© Author(s) 2026. CC BY 4.0 License.

elucidate the detailed tectonic framework of the CITZ and the surrounding adjacent region.

5 Conclusions

This study focuses on mantle deformation beneath the CITZ, supported by SWS data from the Satpura Gondwana region. The key implications of our study are as follows:

1. The SK(K)S splitting results indicate the presence of a significant anisotropic fabric beneath the studied area.
2. The FPDs generally vary from NNE-SSW to ENE-WSW, deviating from the APM direction of the Indian plate ($\sim$48°). The deviation of the averaged FPD orientation from the APM direction of the Indian plate at each seismic station suggests that the inferred deformation pattern is caused by a combination of frozen lithospheric deformation and sub-lithospheric mantle dynamics, rather than asthenospheric flow caused by Indian plate motion. The presence of preserved anisotropic signatures, which have been retained due to the orogenic processes associated with the convergence and collisions of the Northern Bundelkhand and Deccan protocontinents during the evolution of CITZ until the early Neoproterozoic.
3. The lower splitting delay times (δt $<$ 1s) for seismic stations SG02, SG06, SG07, and SG09 can be attributed to plume upwelling during the late Cretaceous to early Paleocene, as indicated by the presence of dykes or their vicinity to the Deccan Trap.
4. The obtained FPD orientation at seismic station (SG08), situated near the Tapti Fault, is aligned with the fault's strike. This suggests that the fault is deep-seated, potentially extending to the lithospheric mantle, and that seismic anisotropy in this area is structurally influenced by the fault, indicating its role as a weak lithospheric zone impacting upper mantle deformation.
5. Variations in splitting patterns indicate the presence of a multilayered anisotropic fabric. However, validation of this interpretation is challenging due to the limited back-azimuthal coverage, which is constrained by India's geographic location and methodological limitations of the RC and SC techniques.

Code and data availability. The SplitLab code used to perform SK(K)S phase splitting measurements is available under a General Public License (GPL) at https://github.com/IPGP/splitlab. The waveform data used in this investigation are available on request from the corresponding author.

Author contributions. Nitarani Bishoyi: Conceptualization, Methodology, Software, Data curation, Visualization, Validation, Writing-Original draft. Arun Kumar Dubey: Data collection, Validation, Writing-Reviewing and Editing. Ashwani Kant Tiwari: Supervision, Conceptualization, Methodology, Visualization, Validation, Resources, Writing-Reviewing and Editing

https://doi.org/10.5194/egusphere-2025-6202
Preprint. Discussion started: 10 February 2026
© Author(s) 2026. CC BY 4.0 License.

Competing interests. The authors declare that they have no conflict of interest.

Acknowledgements. This study was funded by the Indian Institute of Science Education and Research Bhopal. We are thankful to our group members Rahul Kumar, and Rishabh Tripathi for their excellent support during fieldwork and the smooth functioning of the project. We used Generic Mapping tools (Wessel et al., 2013, 2019) to create all figures except Figures 5, 6, and 11. We thank associate editor Irene Bianchi for her valuable comments and suggestions, which helped us to improve the paper substantially.

https://doi.org/10.5194/egusphere-2025-6202
Preprint. Discussion started: 10 February 2026
© Author(s) 2026. CC BY 4.0 License.

References

Acharya, S.: Evolutionary characters of the Gondwanic Indian crust, Indian Minerals, 51, 1–24, 1997.

Acharyya, S.: The nature of Mesoproterozoic Central Indian Tectonic Zone with exhumed and reworked older granulites, Gondwana Research, 6, 197–214, 2003.

Altamimi, Z., Metivier, L., Rebischung, P., Collilieux, X., Chanard, K., and Barnéoud, J.: ITRF2020 plate motion model, Geophysical Research Letters, 50, e2023GL106 373, 2023.

Barruol, G. and Mainprice, D.: A quantitative evaluation of the contribution of crustal rocks to the shear-wave splitting of teleseismic SKS waves, Physics of the Earth and Planetary Interiors, 78, 281–300, 1993.

Bhandari, A., Chandra Pant, N., Bhowmik, S. K., and Goswami, S.: 1.6 Ga ultrahigh-temperature granulite metamorphism in the Central Indian Tectonic Zone: insights from metamorphic reaction history, geothermobarometry and monazite chemical ages, Geological Journal, 46, 198–216, 2011.

Bhowmik, S. K.: The current status of orogenesis in the Central Indian Tectonic Zone: A view from its Southern Margin, Geological Journal, 54, 2912–2934, 2019.

Bhowmik, S. K., Wilde, S. A., Bhandari, A., Pal, T., and Pant, N. C.: Growth of the Greater Indian Landmass and its assembly in Rodinia: geochronological evidence from the Central Indian Tectonic Zone, Gondwana Research, 22, 54–72, 2012.

Bhukta, K., Khan, P. K., and Mandal, P.: Upper mantle anisotropy inferred from shear wave splitting beneath the Eastern Indian Shield region, Geoscience Frontiers, 9, 1911–1920, 2018.

Biswal, S., Kumar, S., Roy, S. K., Kumar, M. R., Mohanty, W., Parija, M. P., and Paul, A.: Upper mantle anisotropy beneath the Western Segment, NW Indian Himalaya, using shear wave splitting, Lithosphere, 2020, 8856 812, 2020.

Bora, S. and Kumar, S.: Geochemistry of biotites and host granitoid plutons from the Proterozoic Mahakoshal Belt, central India tectonic zone: implication for nature and tectonic setting of magmatism, International Geology Review, 57, 1686–1706, 2015.

Bormann, P., Grünthal, G., Kind, R., and Montag, H.: Upper mantle anisotropy beneath central Europe from SKS wave splitting: Effects of absolute plate motion and lithosphere-asthenosphere boundary topography?, Journal of Geodynamics, 22, 11–32, 1996.

Bowman, J. R. and Ando, M.: Shear-wave splitting in the upper-mantle wedge above the Tonga subduction zone, Geophysical Journal International, 88, 25–41, 1987.

Chakraborty, C. and Ghosh, S. K.: Pull-apart origin of the Satpura Gondwana basin, central India, Journal of earth system science, 114, 259–273, 2005.

Chattopadhyay, A., Chatterjee, A., Das, K., and Sarkar, A.: Neoproterozoic transpression and granite magmatism in the Gavilgarh-Tan Shear Zone, central India: Tectonic significance of U-Pb zircon and U-Th-total Pb monazite ages, Journal of Asian Earth Sciences, 147, 485–501, 2017.

Chen, Y., Zhang, Z., Sun, C., and Badal, J.: Crustal anisotropy from Moho converted Ps wave splitting analysis and geodynamic implications beneath the eastern margin of Tibet and surrounding regions, Gondwana Research, 24, 946–957, 2013.

Cochran, E. S., Vidale, J. E., and Li, Y.-G.: Near-fault anisotropy following the Hector Mine earthquake, Journal of Geophysical Research: Solid Earth, 108, 2003.

Copley, A., Mitra, S., Sloan, R. A., Gaonkar, S., and Reynolds, K.: Active faulting in apparently stable peninsular India: Rift inversion and a Holocene-age great earthquake on the Tapti Fault, Journal of Geophysical Research: Solid Earth, 119, 6650–6666, 2014.

https://doi.org/10.5194/egusphere-2025-6202
Preprint. Discussion started: 10 February 2026
© Author(s) 2026. CC BY 4.0 License.

Deshmukh, T. and Prabhakar, N.: Linking collision, slab break-off and subduction polarity reversal in the evolution of the Central Indian Tectonic Zone, Geological Magazine, 157, 340–350, 2020.

Hou, G., Santosh, M., Qian, X., Lister, G. S., and Li, J.: Tectonic constraints on 1.3˜ 1.2 Ga final breakup of Columbia supercontinent from a giant radiating dyke swarm, Gondwana Research, 14, 561–566, 2008.

Jade, S., Shrungeshwara, T., Kumar, K., Choudhury, P., Dumka, R. K., and Bhu, H.: India plate angular velocity and contemporary deformation rates from continuous GPS measurements from 1996 to 2015, Scientific reports, 7, 11 439, 2017.

Jana, N., Singh, A., Tiwari, A. K., Eken, T., Singh, A., Singh, C., and Shankar, U.: Seismic anisotropy and mantle deformation beneath Eastern Ghats Mobile Belt using direct-S waves, Precambrian Research, 360, 106 215, 2021.

Kaila, K. and Krishna, V.: Deep seismic sounding studies in India and major discoveries, Current science (Bangalore), 62, 117–154, 1992.

Kanaujia, J. and Surve, G.: Upper mantle deformation beneath the northeastern part of Indian plate from shear-wave splitting analysis, Geo-Marine Letters, 44, 1, 2024.

Kanaujia, J., Mitra, S., Gupta, S. C., and Sharma, M. L.: Crustal anisotropy from shear-wave splitting of local earthquakes in the Garhwal Lesser Himalaya, Geophysical Journal International, 219, 2013–2033, 2019.

Kreemer, C.: Absolute plate motions constrained by shear wave splitting orientations with implications for hot spot motions and mantle flow, Journal of Geophysical Research: Solid Earth, 114, 2009.

Krishnamurthy, P.: The Deccan Volcanic Province (DVP), India: a review: Part 1: Areal extent and distribution, compositional diversity, flow types and sequences, stratigraphic correlations, dyke swarms and sills, petrography and mineralogy, Journal of the Geological Society of India, 96, 9–35, 2020.

Kumar, M. R. and Singh, A.: Evidence for plate motion related strain in the Indian shield from shear wave splitting measurements, Journal of Geophysical Research: Solid Earth, 113, 2008.

Kumar, M. R., Singh, A., Kumar, N., and Sarkar, D.: Passive seismological imaging of the Narmada paleo-rift, central India, Precambrian Research, 270, 155–164, 2015a.

Kumar, P., Yuan, X., Kumar, M. R., Kind, R., Li, X., and Chadha, R.: The rapid drift of the Indian tectonic plate, Nature, 449, 894–897, 2007.

Kumar, P., Ravi Kumar, M., Srijayanthi, G., Arora, K., Srinagesh, D., Chadha, R., and Sen, M. K.: Imaging the lithosphere-asthenosphere boundary of the Indian plate using converted wave techniques, Journal of Geophysical Research: Solid Earth, 118, 5307–5319, 2013.

Kumar, V. P., Prakasam, K., Rai, S., and Gupta, S.: Upper-mantle anisotropy beneath the south Indian Shield: Influenced by ancient and recent Earth processes, Lithosphere, 7, 108–116, 2015b.

Li, Z.-X., Bogdanova, S., Collins, A., Davidson, A., De Waele, B., Ernst, R., Fitzsimons, I., Fuck, R., Gladkochub, D., Jacobs, J., et al.: Assembly, configuration, and break-up history of Rodinia: a synthesis, Precambrian research, 160, 179–210, 2008.

Mahesh, P., Catherine, J., Gahalaut, V., Kundu, B., Ambikapathy, A., Bansal, A., Premkishore, L., Narsaiah, M., Ghavri, S., Chadha, R., et al.: Rigid Indian plate: constraints from GPS measurements, Gondwana Research, 22, 1068–1072, 2012.

Mall, D., Reddy, P., and Mooney, W. D.: Collision tectonics of the Central Indian Suture zone as inferred from a deep seismic sounding study, Tectonophysics, 460, 116–123, 2008.

Mandal, B., Sen, M. K., and Vijaya Rao, V.: New seismic images of the Central Indian Suture Zone and their tectonic implications, Tectonics, 32, 908–921, 2013.

Melo, B., Assumpção, M., and Team, .-B. P.: Mantle anisotropy and asthenospheric flow around cratons in southeastern South America, Geophysical Journal International, 215, 494–506, 2018.

https://doi.org/10.5194/egusphere-2025-6202
Preprint. Discussion started: 10 February 2026
© Author(s) 2026. CC BY 4.0 License.

Naganjaneyulu, K. and Santosh, M.: The Central India Tectonic Zone: a geophysical perspective on continental amalgamation along a Mesoproterozoic suture, Gondwana Research, 18, 547–564, 2010.

Narula, P., Acharyya, S., and Banerjee, J.: Seismotectonic atlas of India and its environs. Geological Survey of India, 2000.

Paul, A., Hazarika, D., and Wadhawan, M.: Shear wave splitting and crustal anisotropy in the Eastern Ladakh-Karakoram zone, northwest Himalaya, Journal of Asian Earth Sciences, 140, 122–134, 2017.

Radhakrishna, B.: Suspect tectono-stratigraphic terrane elements in the Indian subcontinent, Journal Geological Society of India, 34, 1–24, 1989.

Radhakrishna, B. and Naqvi, S.: Precambrian continental crust of India and its evolution, The Journal of Geology, 94, 145–166, 1986.

Radhakrishna, B. and Ramakrishnan, M.: Archaean-Proterozoic boundary in India, Journal Geological Society of India, 32, 263–278, 1988.

Ramachandra, H. and Roy, A.: Evolution of the Bhandara-Balaghat granulite belt along the southern margin of the Sausar mobile belt of central India, Journal of Earth System Science, 110, 351–368, 2001.

Rao, V. V. and Reddy, P.: A Mesoproterozoic supercontinent: evidence from the Indian shield, Gondwana Research, 5, 63–74, 2002.

Rogers, J. J. and Santosh, M.: Supercontinents in Earth history, Gondwana Research, 6, 357–368, 2003.

Rogers, J. J. and Santosh, M.: Tectonics and surface effects of the supercontinent Columbia, Gondwana Research, 15, 373–380, 2009.

Roy, A. and Prasad, M. H.: Tectonothermal events in Central Indian Tectonic Zone (CITZ) and its implications in Rodinian crustal assembly, Journal of Asian Earth Sciences, 22, 115–129, 2003.

Roy, A., Devarajan, M., and Prasad, M. H.: Ductile Shearing and Syntectonic Granite Emplacement along the Southern Margin of the Palaeo-proterozoic Mahakoshal Supracrustal Belt: Evidence from Singrauli Area, Madhya Pradesh, Journal-Geological Society of India, 59, 9–22, 2002.

Roy, S. K., Srinagesh, D., Saikia, D., Singh, A., and Kumar, M. R.: Seismic anisotropy beneath the eastern Dharwar craton, Lithosphere, 4, 259–268, 2012.

Roy, S. K., Kumar, M. R., and Srinagesh, D.: Mantle deformation beneath India inferred from shear wave splitting, Journal of the Geological Society of India, 97, 1200–1206, 2021.

Roy, S. K., Kumar, M. R., Kanaujia, J., Gupta, S., Singh, B., Mandal, P., and Srinagesh, D.: Insights into the mechanisms forging seismic anisotropy in the upper mantle beneath India, Tectonophysics, 888, 230 454, 2024.

Savage, M.: Seismic anisotropy and mantle deformation: what have we learned from shear wave splitting?, Reviews of Geophysics, 37, 65–106, 1999.

Shukla, G., Mallik, J., and Mondal, P.: Dimension-scaling relationships of Pachmarhi dyke swarm and their implications on Deccan magma emplacement, Tectonophysics, 843, 229 602, 2022.

Shukla, S., Chauhan, H., Yousuf, I., and Ahmad, T.: Bulk rock and mineral chemistry of meta-sediments from Mahakoshal Supracrustal Belt, Central Indian Tectonic Zone: constraints on weathering, provenance, paleoclimate and metamorphism, Journal of Sedimentary Environments, 6, 621–645, 2021.

Silver, P. G. and Chan, W. W.: Shear wave splitting and subcontinental mantle deformation, Journal of Geophysical Research: Solid Earth, 96, 16 429–16 454, 1991.

Singh, A., Jana, N., Tiwari, A. K., Eken, T., Singh, A., and Singh, C.: Direct S-wave derived seismic anisotropy beneath Eastern Ghats Mobile Belt and adjacent Archean cratons: Signature of collision and rifting., in: Geophysical Research Abstracts, vol. 21, 2019.

Singh, J., Chandrakala, K., Singh, A., and Mall, D.: Structure and evolution of Satpura Gondwana Basin over Central Indian Tectonic Zone: inferences from seismic and gravity data, Jour. Indian Geophys. Union, 19, 39–54, 2015.

https://doi.org/10.5194/egusphere-2025-6202
Preprint. Discussion started: 10 February 2026
© Author(s) 2026. CC BY 4.0 License.



Sivaram, K., Kumar, V. P., Gupta, S., Prasad, B., and Kumar, S.: Upper mantle seismic anisotropy beneath the Deccan Volcanic Province and the adjacent Eastern Dharwar Craton in south Indian shield from shear wave splitting analysis, Physics of the Earth and Planetary Interiors, 322, 106 829, 2022.

Tewari, H.: A tectonic model of the Narmada region, Current Science, 80, 873–878, 2001.

Vinnik, L. P., Farra, V., and Romanowicz, B.: Azimuthal anisotropy in the Earth from observations of SKS at Geoscope and NARS broadband stations, Bulletin of the Seismological Society of America, 79, 1542–1558, 1989.

Wessel, P., Smith, W. H., Scharroo, R., Luis, J., and Wobbe, F.: Generic mapping tools: improved version released, Eos, Transactions American Geophysical Union, 94, 409–410, 2013.

Wessel, P., Luis, J. F., Uieda, L. a., Scharroo, R., Wobbe, F., Smith, W. H., and Tian, D.: The generic mapping tools version 6, Geochemistry, Geophysics, Geosystems, 20, 5556–5564, 2019.

Wüstefeld, A., Bokelmann, G., Zaroli, C., and Barruol, G.: SplitLab: A shear-wave splitting environment in Matlab, Computers & Geosciences, 34, 515–528, 2008.

Yang, H., Peng, H., and Hu, J.: The lithospheric structure beneath southeast Tibet revealed by P and S receiver functions, Journal of Asian Earth Sciences, 138, 62–71, 2017.

Yedekar, D., Jain, S., Nair, K., and Dutta, K.: The central Indian collision suture, Visesa Prakasana-Bharatiya Bhuvaijñanika Sarveksana, pp. 1–43, 1990.

Zhao, G., Sun, M., Wilde, S. A., and Li, S.: A Paleo-Mesoproterozoic supercontinent: assembly, growth and breakup, Earth-Science Reviews, 67, 91–123, 2004.